Low-level control of actuator for robotic finger

TTK4551 - Engineering Cybernetics, Specialization Project
In collaboration with: SINTEF Ocean

Ruben Winsjansen
Supervised by: Øyvind Stavdahl and Aleksander Eilertsen

4th June 2019

Abstract

As a sub-problem of creating a low-cost open source dexterous hand suitable for handling food, a solution is proposed for low-level control and choice of actuators for a single robotic finger.

Based on the performance stats w/kg and $torque/kg$, and the fact that the system has a weight limit, hydraulic, pneumatic and electromagnetic actuators were the best alternatives for actuation. An electromagnetic actuator (BLDC motor) was chosen based on being a widely available actuator with back driving capability and also well suited for applications that require high accuracy.

The actuator was chosen to have human-like torque capabilities, to ensure that it could pick up items that humans can pick up. The result was a 15W motor with 1/30 gear ratio.

With the introduction of reduction gears, it was shown that elasticity, backlash and friction had a negative impact on the dynamics of the system, making both high and low level control harder.

Planetary gears were shown to be a suitable "off the shelf" alternative, but to further tackle the problem, a custom reduction gear was designed with the intent of minimizing the negative factors. In addition to this, a collection of control based compensation methods were provided in case problems should still arise when the system is tested.

A PI torque controller with trapezoidal commutation was acquired to be used as the low level control system. It was chosen because controllers with trapezoidal commutation are cheap. Field oriented control were suggested as a more expensive alternative in case trapezoidal commutation did not yield the wanted response.

Project assignment

Pick and place operations involving compliant objects still lag behind on implementation. Interaction with pliable and easily damageable materials, such as food, is still a human operated task. To facilitate a transition to robotics within food industries, robots need to be able to gain higher manipulation skills – on par with or beyond human abilities. Dexterity, defined as the ability of hand or end effector to relocate objects in an arbitrary way according to a given task, will be key to enable this shift. Manipulations are defined as dexterous when multiple fingers cooperate to grasp or manipulate an object.
In this assignment, the candidate will work along researchers at SINTEF Ocean and NTNU to build an end effector with proprietary novel sensor technology. In this project you shall start developing a finger for the described system.

1. Sett deg inn i litteraturen rundt bevegelige finger for robotanvendelser, og gi en kort oversikt over de viktigste alternativene med hensyn på aktuatorer og lavnivåregulering av disse. (Perform research into robotic fingers, and provide a brief overview of the most important alternatives in actuator systems and the low level control systems available.)

2. Sett opp en funksjonsspesifikasjon for aktuatorløsningen til det foreliggende prosjektet. Ta hensyn til føringer fra andre deler av prosjektet. (Provide the functional specifications of the system)

3. Velg aktuator- og reguleringsstrategi basert på funnene i punktene over, og konstruer et system som tilfredsstiller funksjonsspesifikasjonen. (Choose an actuator solution and control strategy based on the points above, and design a system that fulfills the functional specifications.)

4. I den grad tiden tillater det, test ut kritiske deler av designet i form av en fysisk modell eller prototyp. (If there is time, test critical parts of the design using a physical model or prototype.)

Contents

1 Introduction **1**
- 1.1 Functional specifications . . . 1
- 1.2 Dexterous manipulation and low-level control . . . 2

2 Actuator alternatives **3**
- 2.1 Electromagnetic actuators . . . 3
- 2.2 Pneumatic actuators . . . 5
- 2.3 Hydraulic actuators . . . 5
- 2.4 Choice of actuator type . . . 6
- 2.5 Tendons . . . 6

3 Choosing a suitable motor **7**
- 3.1 Actuator capabilites . . . 7
- 3.2 Geared or direct-drive . . . 7
- 3.3 Motor choice . . . 8

4 Low level control **11**
- 4.1 Cascade control . . . 12
- 4.2 The inner loop . . . 12
- 4.3 Commutation . . . 13
  - 4.3.1 Nonlinear BLDC-motor model . . . 14
  - 4.3.2 Trapezoidal commutation . . . 16
  - 4.3.3 Sinusoidal commutation . . . 16
  - 4.3.4 Field oriented Control . . . 19
  - 4.3.5 Choice of commutation strategy . . . 20

5 Friction, elastisity and backlash **21**
- 5.1 Friction . . . 21
  - 5.1.1 Integral control with deadband . . . 23
  - 5.1.2 Dither . . . 23
  - 5.1.3 Impulsive control . . . 23
  - 5.1.4 Friction Feedforward/Feedback . . . 23
  - 5.1.5 Adaptive Feedforward/Feedback . . . 23
  - 5.1.6 Joint Torque control . . . 24

5.2 Elasticity 24
5.3 Backlash 24

6 Choosing a suitable reduction gearbox **27**
6.1 Custom transmission system based on pulleys 28
6.1.1 Design philosophy 30
6.1.2 Similar concepts 30
6.2 Gear choice 30

7 Conclusion and future work **31**
7.1 Conclusion 31
7.2 Future work 31

Bibliografi **35**

A Datasheet for BLDC motor **a**

B Datasheet for PI torque controller (Trapezoidal commutation) **c**

C Blueprints for custom transmission system **g**

Chapter 1

Introduction

As a sub-problem of creating a low-cost open source dexterous hand suitable for handling food, a solution is proposed for low-level control and choice of actuators for a single robotic finger.

We begin by listing the specifications of the hand, define the meaning of dexterous manipulation, and what requirements it puts on the low level control system.

1.1 Functional specifications

The following specifications is intended for the gripper as a whole, and will influence the requirements for the low level control system of the finger. They are based on conversations and meetings with the project supervisor at SINTEF Oscean, Aleksander Eilertsen.

- Dexterous
- Two actuated joints. One passive joint.
- Cheap
- Easy to repair
- Widely available components
- Max weight(gripper + object) for prototype: 3kg
- Impulse control or back driving capability to avoid damage from collision
- Suitable for handling food
- Able to manipulate objects like apples, tomato's and small fish.
- The strength of the finger is not particularly important for the prototype so long as the system is scalable. However, for the tasks above, Albert Danielsen estimated a maximum load of 700g (1).

The tip of the finger will be equipped with a Gelsight sensor (2) which measures its own deformation in contact with an object at a rate of 30 measurements per second. It is important that considerable readjustments in applied force can be made between measurements to prevent the object from slipping. Specifically; A 30% increase in applied force in $\frac{1}{30}$s. The finger joint should also be able to move through its whole range of motion within a second.

1.2 Dexterous manipulation and low-level control

Okamura, Smaby and Cutkosky defined dexturous manipulation as a field of robotics in which multiple grippers or fingers cooperate to grasp and manipulate objects (3). As an example, they presented a typical dexterous manipulation problem where several manipulators cooperate to change the configuration of an object while maintaining contact throughout the manipulation (3).

In this paper, the term *low level control* refers to the force/torque control of the actuator system. From the description of dexterous manipulation it is evident that it is important that commands are carried out precisely as planned to not hinder collaboration. Thus, precision and accuracy to the extent that it does not hinder the finger in following a trajectory is a requirement.

Chapter 2

Actuator alternatives

An Actuator is a device which turns a control signal into mechanical action (4). For the joints of a robotic finger the desired mechanical action is to apply a torque around the joint axis. While conventional electrical motors provide this type of action directly, others options such as linear motors, pneumatic or hydraulic pistons, and various types of artificial muscles (5) provide the same functionality through tendons connected to levers and pulleys.

Since it is specified that the components should be widely available, the more exotic actuators like artificial muscles can be excluded immediately. Furthermore, there is a weight limit, and electromagnetic, pnaumatic and hydraulic actuators, offer the best performance in W/kg (6), and is known to be viable for robotics (6).

2.1 Electromagnetic actuators

Electromagnetic actuators offers the best performance in position accuracy (7), and are commonly used in robotics (6). Common types of small electromagnetic actuators for robotics are stepper motors, brushed DC-motors and brushless DC-motors (BLDC).

Stepper motor

In a stepper motor, a full rotation is divided into a series of steps. The motor can hold still at a step, or move to the next or previous step. The position of a stepper motor can be accurately controlled without feedback simply by counting the steps taken from the initial position. The initial position can be stored, calibrated on start-up, or measured with an absolute encoder. If external forces causes it to slip, the motor has to be re-calibrated.

Advantages

- Cheap.
- Widely available as a complete system with reduction gear and controller, and therefore extremely easy to set up

- High torque at low speeds

Disadvantages

- Hard to control torque.
- Low positional resolution.
- Jittery movement at low speeds because of resolution.
- No backdrivability

Brushed DC-motor

Although there are serveral configurations, a simple brushed DC-motor typically has a permanent magnet stator, and rotor coil powered through two brushes. One at each side of the rotor. When powered, the coil produces a magnetic field, causing the rotor to rotate to align itself with the stator field. After a 180 degree rotation, the brushes has changed places, and the polarity of the coil is reversed. This process is called commutation, and keeps the rotor going.

Advantages

- Old and proven technology
- Simple

Disadvantages

- Parts that wear out
- Dust from brush
- Less efficient than BLDC

Brushless DC motor

The brushless DC motor has a permanent magnet rotor, and a stator coil. Unlike the DC-motor, there are no brushes, in therefore also no inherent capability to change the direction of the field throughout the rotation. BLDC motors has to be commutated electronically, which adds to the complexity. However, this means less friction, and no parts that wears out.

Advantages

- No parts that wear out (except bearings)
- Highly efficient

Disadvantages

- Must be electronically commutated

2.2 Pneumatic actuators

Pneumatic actuators often come in the form of pistons or air motors and is powered by pressurized air controlled with valves. Pneumatic actuators is often used as a cheaper, safer and more flexible alternative to electromagnetic actuators (8). They are also incredibly fast (9). Pneumatic actuators are used in robotics (6), including projects similar to our project (10).

Advantages

- Outperform hydraulic and electromagnetic actuators in speed. (9)
- Outperform electromagnetic actuators in torque density (6)
- No gears or pulleys needed.
- Does not overheat, 100% duty cycle.
- Safe in hazardous and flammable areas.
- Power source does not need to be mounted on robot

Disadvantages

- Loud (9)
- Low efficiency compared to electromagnetic actuators (9)
- Difficult to control position accurately (9)

2.3 Hydraulic actuators

Hydraulic actuators transform energy in the form of a pressurized fluid into linear or rotary motion. In the same way as pneumatic actuators, they often come in the form of pistons and hydraulic motors. They are popular for large machinery (E.g. Excavators). When pure strength is the main objective, hydraulic actuators are a natural choice. Hydralic actuators have also been used in projects similar to our project (11).

Advantages

- Outperform electromagnetic and pneumatic actuators in torque and power density (6)
- No gears or pulleys needed.
- Power source does not need to be mounted on robot

Disadvantages

- Risk of leakage
- Lack of backdrivability for force control (6), Although there are workarounds (12).
- Low efficiency compared to electromagnetic actuators (9)

2.4 Choice of actuator type

Every actuator listed above is proven to be viable for robotics, and neither are particularly bad. For every problem listed as a disadvantage, there are multiple solution available. The stepper motor is excluded because of the difficulty in controlling torque, and lack of back driving capability. The brushed DC-motor is worse than BLDC in almost every way except ease of use. Dust from brush wear can also be problematic in areas where food is handled. A hydraulics leak would also be problematic around food, and could take a while to notice in a fully autonomous robot cell. Since electromagnetic actuators offer the highest accuracy in positioning (7), and there are no requirements for extreme strength or acceleration or speed, the BLDC-motor is a suitible choice based on the specifications.

2.5 Tendons

Whether or not to use tendons for this project has also been discussed (1) from a design perspective, with the conclusion that tendons is the correct choice. For low level control, the main advantage of tendons is the ability to place the actuators outside the finger. This reduces the weight of the finger significantly, and thus also the moment of inertia around the joint axis. This increases the bandwidth of the system. The disadvantages of tendons is that the design is more complicated, and the introduction of additional unwanted dynamics caused by the flexibility of the tendon. Depending on how the tendons are routed from the actuator to the joint, they may also cause additional friction. Nevertheless, we have decided to use tendons for this project.

Chapter 3

Choosing a suitable motor

As mentioned in the specifications, there are no specific torque or power output requirements for the end effector. So long as the concept is scalable, a larger version can be produced.

3.1 Actuator capabilites

We know the end effector should be able to handle small objects like tomatoes and apples. Since the human hand is able to perform these tasks and more, the robot hand should at best be equally strong and at least be able to deliver torque in the same order of magnitude. At this stage we don't know how many fingers the manipulator will end up with, so it is better to make it too strong.

For the average human, the muscle driving the flexor tendon of the inner joint of the middle finger is able to provide 118N. With a lever arm of 0.8cm, the driving torque is 0.8Nm (13). The next joint is slightly weaker with 105N, and 0.4cm lever arm giving 0.6Nm torque. Using these values as an upper limit, we can begin have a rough idea of the capabilities

3.2 Geared or direct-drive

Providing the same torque as a human finger from an electrical motor is not practical without gear reduction. It would typically require at least a 200W motor to produce the same torque continuously. Unfortunately, gears have a negative impact on the dynamics system because of friction, elasticity, and backslash. These problems will be discussed in chapter 5. To choose a suitable motor, we need a rough idea of the transmission ratio. High reduction ratio reduces back driving capabilities (14) because of friction in the gearbox (15) which is higher from the driven side. This means that we can't choose a weak motor with extremely large transmission ratio. Maxon motors (16) delivers a wide range of BLDC motors and gearboxes, where the transmission ratio ranges from around 1/4 to 1/370. Choosing a transmission ratio of 1/30 would therefore be on the low end, and

require a motor with continuous torque of 27mNm to provide torque equal to a human finger. Note that human torque capabilities is the upper limit for what we require, and that a lower transmission ratio can be chosen later for better back driving capabilities.

3.3 Motor choice

Two 24V 15W maxon EC flat BLDC motors were bought for the project. They have a max continuous torque output of 25.5mNm, which is reasonably close to what we need. A no-load speed of 4530 rpm, and a flat design which is easier to work with. The data-sheet for the motor is available in appendix A.

According to the specifications, the actuator was required to cause significant increase in torque in between measurements of the Gelsight sensor, and the full range of motion has to be performed in under a second. The measurement interval is seen in equation (3.1a). The settling time for a first order system after being subject to a unit step is roughly 5 times the time constant (T). The time constant is calculated in equation (3.1b), and it is seen in equation (3.1c) that the requirement is fulfilled by a large margin.

$$t = \frac{1}{30} = 33,3 \cdot 10^{-}3 \tag{3.1a}$$

$$T = \frac{L}{R} = \frac{0.00772H}{13.8\Omega} = 5.59 \cdot 10^{-4} \tag{3.1b}$$

$$5T = 2.80 \cdot 10^{-3} < t \tag{3.1c}$$

Figure 3.1 shows the result of a simulation with a linear motor model (figure 4.1). In the simulation, the motor is supplied with 24V, the current is limited to 0.5A. With a reduction ratio of 30, the full range of motion is approximately $0.25 \cdot 30 \cdot 2\pi = 47rad$, and is traveled in 1 second with a load inertia of $0.23kgm^2$. The inertia of the finger and gear is not decided yet, but is expected to be much lower. Thus, the speed requirement is fulfilled.

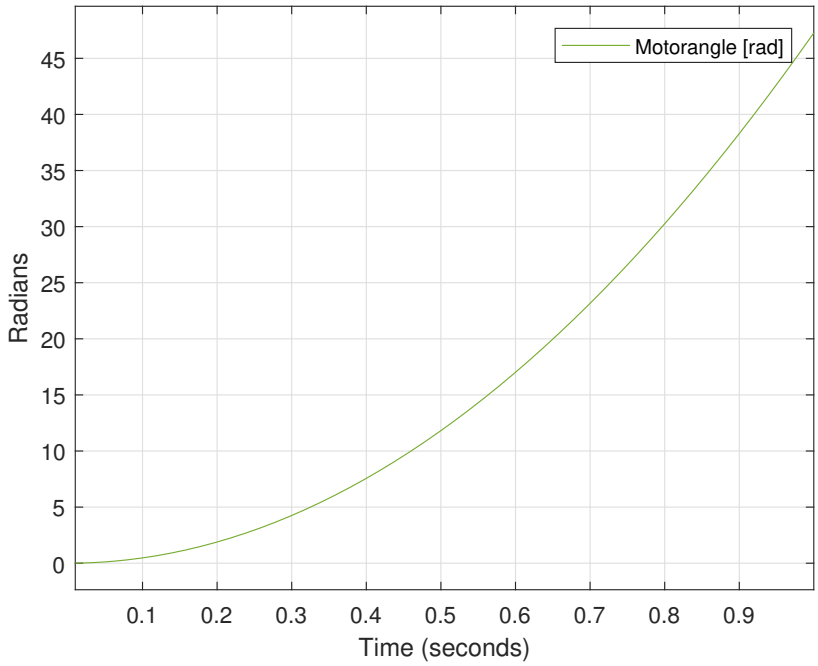

Figure 3.1: Simulated travel through the whole range of motion

Chapter 4

Low level control

The complex tasks performed by a robot a relies on the servo motors being able to perform some basic tasks; Applying the correct torque, moving to a certain position (and staying there), and following a trajectory. In this paper, torque control is referred to as ”low level control”. However, the reduction gear is part of the scope of this paper, and affects the higher level control. Therefore some information about high level control will be provided in chapter 5.

In this chapter we begin by defining a basic model and control structure for reference, and then look at a nonlinear motor model and choose a low level control strategy.

The reference system is based on a linear model of a brushed DC-motor (equation 4.1). Equation (4.1a-4.1b) represents the electrical circuit where *u* is the applied voltage, *R* is the winding resistance, *i* is the current, *L* is the winding inductance, *e* is the back EMF, and ω is the rotational velocity. Equation (4.1c-4.1d) represents the mechanical system where J_m is the rotor inertia, J_l is the load inertia, *B* is the friction coefficient, τ_e is the produced torque, and τ_l represents the disturbances from the load.

$$u = Ri + \frac{di}{dt}L + e \tag{4.1a}$$

$$u = Ri + \frac{di}{dt}L + \frac{1}{K_v}\omega \tag{4.1b}$$

$$(J_m + J_l)\frac{d\omega}{dt} + B\omega = \tau_e - \tau_l \tag{4.1c}$$

$$(J_m + J_l)\frac{d\omega}{dt} + B\omega = K_t i - \tau_l \tag{4.1d}$$

The motor velocity constant K_v and the torque constant K_t can be derived by assuming electrical power minus losses is equal to mechanical power produced by the motor (4.2a-

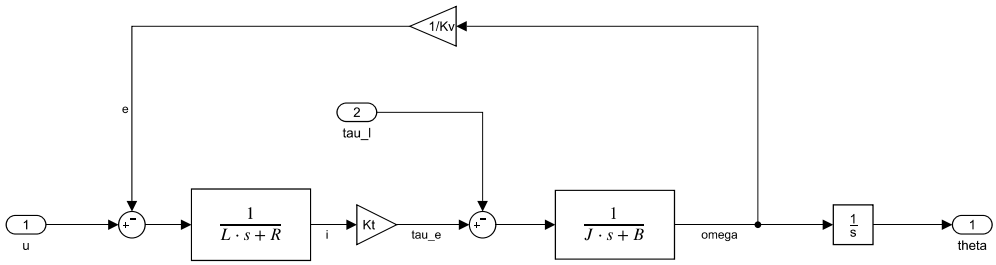

Figure 4.1: Block diagram of the brushed DC-motor

4.2c). The block diagram of the system (4.1b) and (4.1d) is seen in figure 4.1.

$$P = ei = \omega\tau_e \tag{4.2a}$$

$$\frac{e}{\omega} = \frac{\tau_e}{i} \tag{4.2b}$$

$$\frac{1}{K_v} = K_t \tag{4.2c}$$

4.1 Cascade control

A common approach to control a motor is to separate the the control system into an inner and outer loop (17). This strategy is called *Cascade control*, and a block diagram is shown in figure 4.2. The inner loop controls the current/torque, and the outer loop commands the required torque to attain a position or follow a trajectory (high level control). There are two main advantages to this strategy; Disturbances in the inner loop can be corrected fast before they propagate to the outer loop, and since the inner loop settles so much faster than the outer loop, we can approximate the transfer function of the inner loop as a constant when analyzing the outer loop. This reduces the control problem into two smaller problems. By using this method of nested loops, even an advanced system like the autopilot of an aircraft can be reduced to simple control problems (18).

The inner loop must be at least 4-10 times faster (higher bandwidth) than the outer loop, and a pole placement strategy is therefore the natural tuning strategy. However, the response of the electrical circuit is typically so much faster than the mechanical system (17) that a manual tuning strategy like Ziegler–Nichols (19) method should yield sufficient bandwidth separation.

4.2 The inner loop

For the inner loop, the back EMF e is considered a disturbance. Since torque is proportional to current in the linear model, either one can be used as feedback for the inner loop. Getting accurate current measurements is generally easier than torque measurements. On the other hand, torque measurements can to some extent be made after friction losses, which we will later see is an advantage. For the reference control system, we will be using

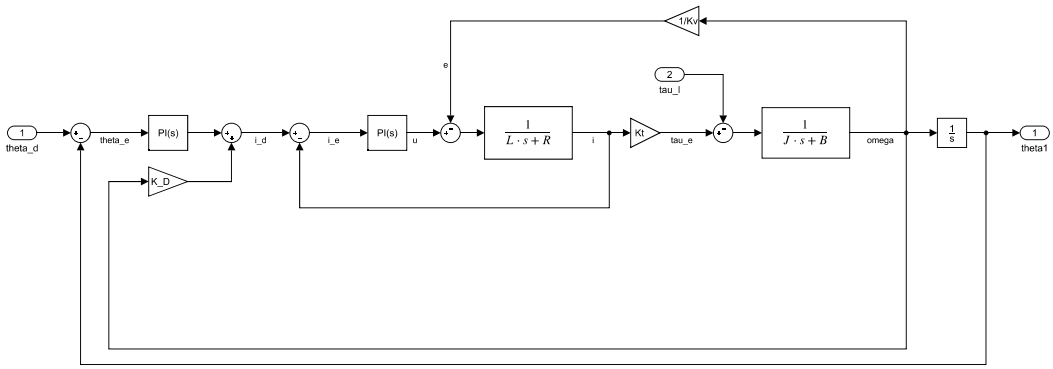

Figure 4.2: Block diagram of the brushed DC-motor with cascade control

current feedback. The linear model of the electrical circuit with back EMF as a disturbance is a first order system, and is easily stabilized by a PID controller. The derivative term gives us a more aggressive system, but is not strictly necessary. Unless we measure it directly, it requires calculating the derivative of the measured current, which amplifies noise. For the reference control system it is therefore not included. The integral term is also not always necessary as long as there is an integral term in the outer loop. Integral control should be used if controlling torque is a goal in itself, and if steady state errors in torque pose a problem. For example, the impact of a feed-forward input from the outer loop is dependant on the inner loop producing the correct torque. In robotics, feed-forward is commonly used to counteract gravitational forces since the robot is heavy, rigid, and the positions of the links are known with high accuracy. Therefore we decided on a PI controller for the inner loop.

4.3 Commutation

The linear model in equation (4.1a-4.1d) is based on a brushed DC-motor. The BLDC-motor however has three phases, and are more similar to a permanent magnet synchronous motors. The key difference is that synchronous motors generate sinusoidal back EMF, while a BLDC motor generates trapezoidal EMF (20). This is because the BLDC-motor is designed to be driven by coordinated steps of DC-current which coincides with the flat top and bottom part of the back EMF curve, to produce torque independent of rotor position. The process of coordinating the current in relation to the back EMF is called *commutation*.

In this section we will use a nonlinear BLDC-motor model to show why the brushed DC-motor model is a good approximation of a commutated BLDC-motor. We will also discuss different commutation strategies.

4.3.1 Nonlinear BLDC-motor model

The voltage balance of each winding is shown in equation (4.3a)-(4.3c), where R is the phase resistance and L is the phase inductance. u_a, u_b and u_c is the phase voltage. i_a, i_b and i_c is the phase current. e_a, e_b, and e_c is the trapezoidal back EMF given by equation (4.4a)-(4.4b) (21).

$$u_a = Ri_a + \frac{di_a}{dt}L + e_a \tag{4.3a}$$

$$u_b = Ri_b + \frac{di_b}{dt}L + e_b \tag{4.3b}$$

$$u_c = Ri_c + \frac{di_c}{dt}L + e_c \tag{4.3c}$$

The back EMF is dependant on both the electrical angle θ_e and rotational speed ω_e of the rotor field, and can be seen in figure 4.3. λ is the torque constant, which is analogous to K_t in equation (4.2c).

$$\begin{bmatrix} e_a \\ e_b \\ e_c \end{bmatrix} = \lambda\omega \begin{bmatrix} f(\theta) \\ f(\theta + \frac{2\pi}{3}) \\ f(\theta - \frac{2\pi}{3}) \end{bmatrix} \tag{4.4a}$$

$$f(\theta) = \begin{cases} \theta\frac{6}{\pi} & 0 \leq \theta < \frac{\pi}{6} \\ 1 & \frac{\pi}{6} \leq \theta < \frac{5\pi}{6} \\ (\pi - \theta)\frac{6}{\pi} & \frac{5\pi}{6} \leq \theta < \frac{7\pi}{6} \\ -1 & \frac{7\pi}{6} \leq \theta < \frac{11\pi}{6} \\ (\theta - 2\pi)\frac{6}{\pi} & \frac{11\pi}{6} \leq \theta < 2\pi \end{cases} \tag{4.4b}$$

The electrical and mechanical power balance (4.5a) is used to derive the torque equation, which can be expressed as (4.5b) or (4.5c) (21).

$$P = \omega\tau_e = e_a i_a + e_b i_b + e_c i_c \tag{4.5a}$$

$$\tau_e = \frac{e_a i_a + e_b i_b + e_c i_c}{\omega} \tag{4.5b}$$

$$\tau_e = \lambda[f(\theta)i_a + f(\theta + \frac{2\pi}{3})i_b + f(\theta - \frac{2\pi}{3})i_c] \tag{4.5c}$$

From equation (4.5c) we see that the torque produced throughout an electrical rotation depend on both current and rotor position.

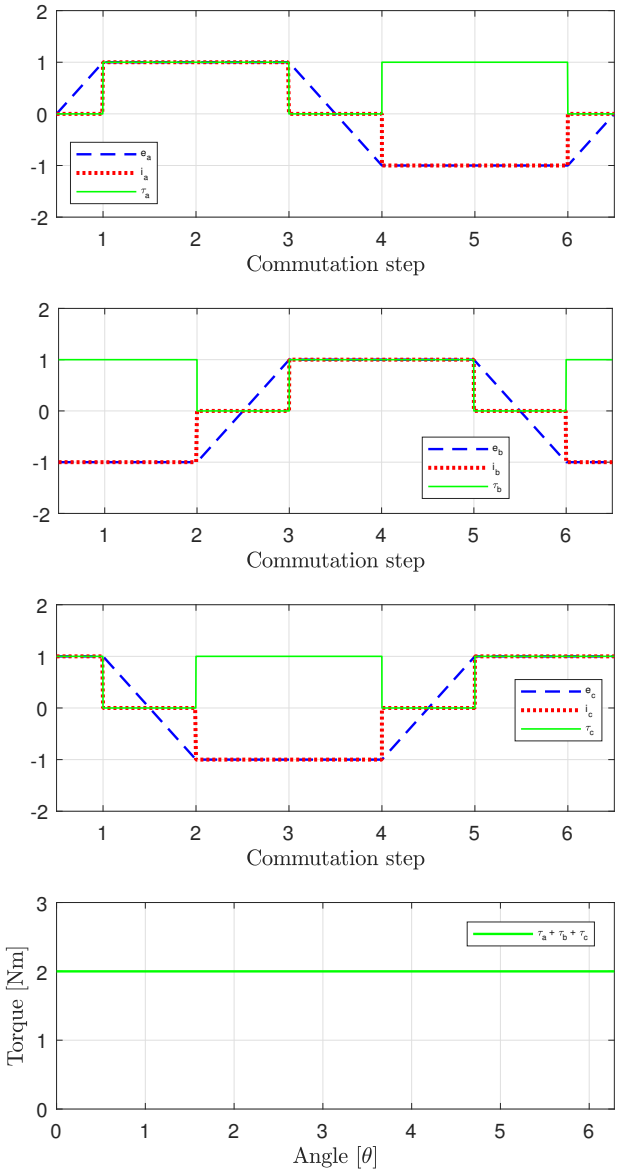

Figure 4.3: BLDC commutation principle

4.3.2 Trapezoidal commutation

BLDC motors are commutated or *switched* electronically, so that each winding receive DC current periodically depending on rotor position. The position is often measured by hall sensors which changes value at each commutation step. One electrical rotation is divided into 6 commutation steps. The position can also be estimated based on back EMF (22), but the start up can be sluggish, and the accuracy is reduced on low speeds (22). Because the phase current is not continuous, the trapezoidal commutation concept is best described graphically, and is depicted in figure 4.3. From the figure it can be seen that the current coincide with the top and bottom part of the back EMF curve, and is zero otherwise. Two windings produce torque at any point during the rotation, while one remain idle. From equation (4.5c) we see that this causes the sum torque to be constant with respect to rotor angle in the same way as in a brushed DC-motor. It is the trapezoidal shape of the back EMF which enables the motor to produce constant torque with pulses of DC-current.

In practice the inductance of the windings limit the rate of change of the current, and it cannot be instantly switched on or off. At the moment of commutation, the current/torque given by a winding that has just been switched on is rising, while the torque produced by another winding that has just been switched off is falling. A miss-match between the upward and downward slope of the phase currents gives rise to a phenomena called *commutation torque ripple* (23). At high speeds the downward slope is steepest, resulting in decreased torque at the commutation points. The phase current is therefore often depicted as gradually increasing when switched on, but instantly set to zero when turned off when the commutation concept is illustrated. At low speeds, small torque spikes occur at the commutation points instead.

The advantage of trapezoidal BLDC controllers is that they are cheap, easy to set up, and widely available. The drawback is the torque ripple.

4.3.3 Sinusoidal commutation

Synchronous motors, which is similar to the BLDC motor, is driven by alternating current and does not need to be commutated. By replacing the trapezoidal function $f(\theta)$ with a sine function, we get the torque equation for synchronus motors. Equation (4.6a)-(4.6c) shows that a constant torque is produced when a sinusoidal current is applied in phase with the back EMF of a synchronous motor.

$$f(\theta)i_i(\theta) = sin^2(\theta) \rightarrow \tag{4.6a}$$

$$\tau_e = \lambda[sin^2(\theta) + sin^2(\theta + \frac{2\pi}{3}) + sin^2(\theta - \frac{2\pi}{3})] \tag{4.6b}$$

$$\tau_e = \lambda \cdot 1.5 \tag{4.6c}$$

We see from equation (4.6a)-(4.6c) that the torque also varies depending on the phase ϕ between current and back EMF. However, for a synchronous motor there is no ripple even

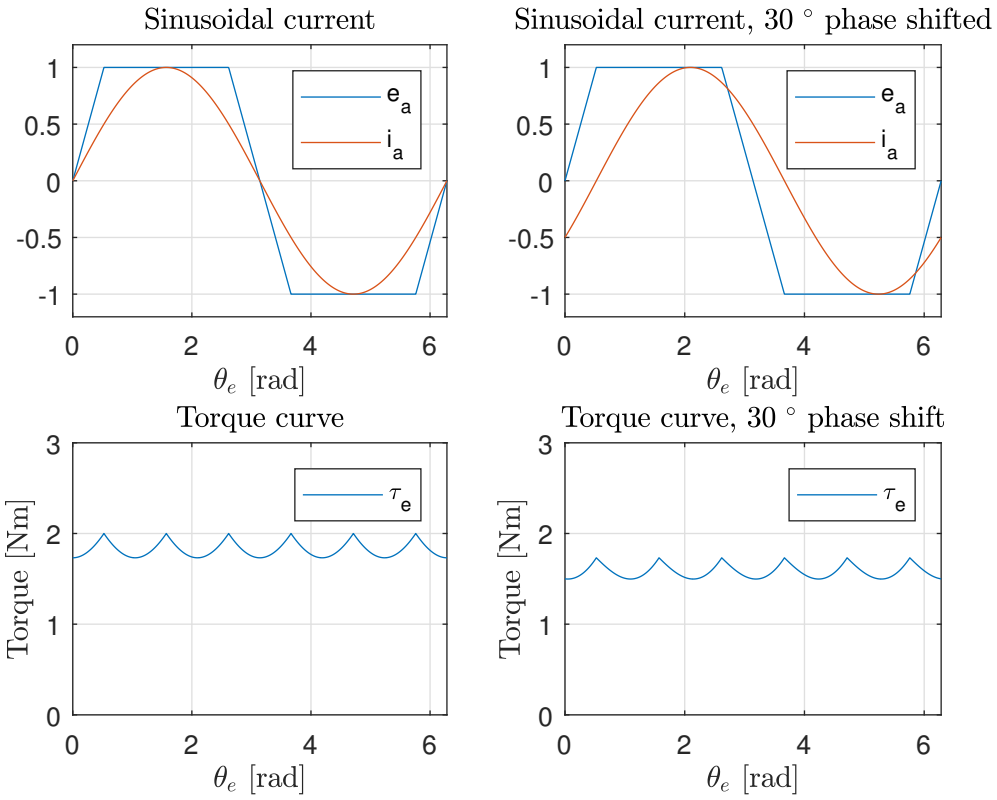

Figure 4.4: Resulting torque with respect to angle created by sinusoidal current waveform on BLDC motor

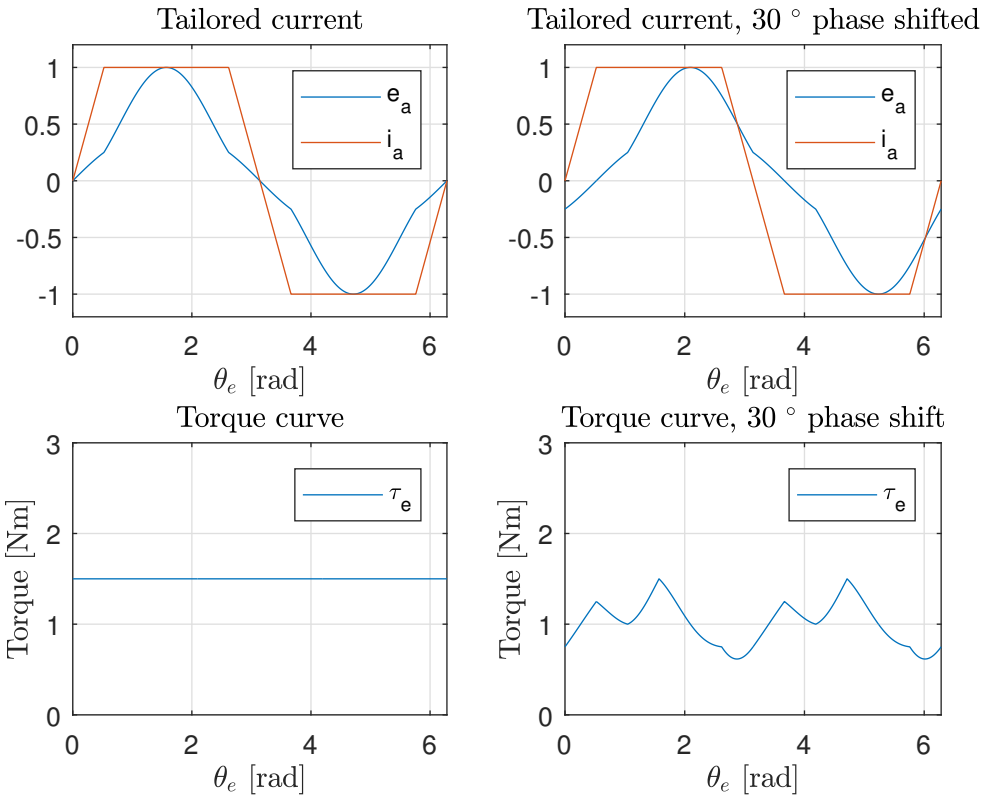

Figure 4.5: Resulting torque with respect to angle created by a current waveform tailored for the rotor field of a BLDC motor

though the current is not in phase.

$$f(\theta)i_i(\theta) = sin(\theta)sin(\theta + \phi) \rightarrow \quad (4.7a)$$

$$f(\theta)i(\theta) = sin^2(\theta)cos(\phi) + sin(\theta)sin(\phi)cos(\theta) \quad (4.7b)$$

$$f(\theta)i(\theta) = sin^2(\theta)cos(\phi) + \frac{sin(2\theta)}{2}sin(\phi) \quad (4.7c)$$

$$\tau_e = \lambda[1.5cos(\phi) + [sin(2\theta) + sin(2(\theta + \frac{2\pi}{3})) + sin(2(\theta - \frac{2\pi}{3}))]\frac{sin(\phi)}{2}] \quad (4.7d)$$

$$\tau_e = \lambda \cdot 1.5 \cdot cos(\phi) \quad (4.7e)$$

To reduce torque ripple, BLDC motors are sometimes driven with sinusoidal voltage which in turn produces sinusoidal current (at low speeds). This method requires position measurements with high resolution and frequency. The torque produced from sinusoidal currents can be seen in figure 4.4. Since the back EMF profile is not sinusoidal, the torque is not completely smooth in this case either, even if the current is perfectly sine shaped. A current waveform which produces smooth torque is displayed in figure 4.5. However, any phase shift results in ripple, and the back EMF profile would have to be measured very precisely to calculate the optimal current waveform. The result in figure 4.4 show that the torque ripple from a sine shaped current does not significantly increase in magnitude with phase shift, but the average toque and therefore also the efficiency is reduced.

At high speeds, a high frequency voltage signal must be applied to the circuit, and therefore phase shift and the reduction in efficiency is inevitable. The back EMF is proportional to angular velocity, and will also begin to distort the voltage applied to the windings, which in turn distorts the current waveform. Sinusoidal commutation is therefore best suited for low speed applications. Although i have found this commutation method described online (24), i have not found a commercial version advertised for BLDC motors. However, a controller advertised for *permanent magnet synchronous motors* uses the same principle, or potentially *field oriented control* if it's a high end controller. Both method works for a BLDC-motor.

4.3.4 Field oriented Control

A popular solution for high performance servoing is *Field oriented Control* (25). A block diagram of the control strategy is seen in [(26) fig. 4.6] where measurements of phase currents and electrical angle is transformed with the Park and Clarke transform, into two currents; The current in phase with the rotor field I_d, and the current 90 degrees phase shifted from the rotor field I_q. Torque is highest when the stator and rotor field are 90 degrees phase shifted, so a control loop is implemented to drive I_d to zero while I_q is set according to the needed torque by applying a voltage signal in the same coordinate frame (voltage in phase with rotor field v_d and voltage out of phase v_q). The inverse transformation of this voltage signal yields the phase voltages which is applied to the motor.

This method is efficient at any speed since the phase shift between current and back EMF is eliminated. The commutation torque ripple is minimal. It is also several times more expensive than the trapezoidal drive. It requires low latency and high frequency

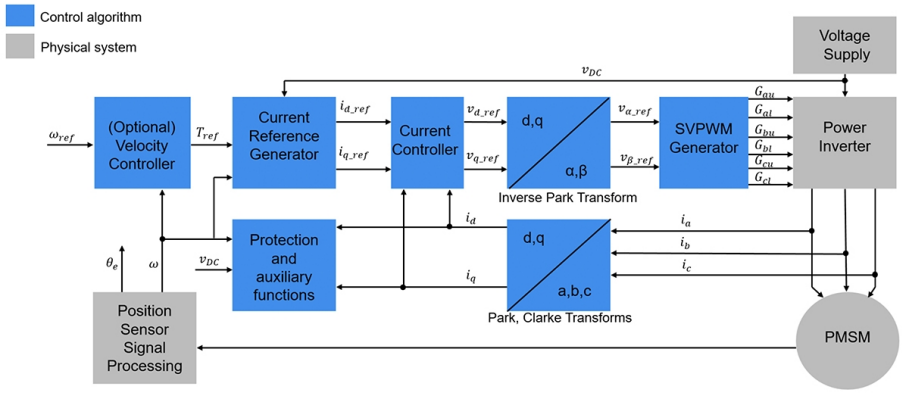

Figure 4.6: Block diagram of field oriented control

measurements of both position and currents. Maxon motors recommends a resolution of 2000 points per revolution for encoders used in field oriented control or sinusoidal commutation (27). The computational load for processing these high frequency measurements is quite high compared to the trapezoidal commutation approach.

4.3.5 Choice of commutation strategy

The benefits of sinusoidal commutation (low torque ripple at very low speeds), does not quite outweigh the drawbacks (low efficiency and high torque ripple at high speeds). Thus, the decision was made to test a trapezoidal commutation driver, and decide if field oriented control is necessary to achieve the requirements set in chapter 1.2.

The controller *ESCON Module 24/2, 4-Q servo controller for DC/EC motors, 2/6 A, 10-24 VDC* (Appendix B) was ordered 4.10.2018 to test whether the commutation ripple was detrimental to the control system. However, there were no time for testing since it arrived over one month later during the exam period (11.14.2018). During the waiting period, significant time went instead into the choice of reduction gear, which continued after the arrival of the driver.

The choice of commutation method is therefore not yet final. However, the potential pitfalls and solutions have been identified. Furthermore, since the design of the end effector (1) has been developed simultaneously with this project, a more conclusive test of the performance of the trapezoidal drive can be made in the continuation of this project. Finally, the transfer function between torque and angular velocity (equation 4.8) is a low-pass filter, which indicates that commutation ripple should not be a significant problem.

$$H(s) = \frac{1}{J \cdot s + B} \tag{4.8}$$

Chapter 5

Friction, elastisity and backlash

In chapter 3.2 it was mentioned that the elasticity, friction and backlash introduced by the reduction gear has a negative impact on dynamics of the system. In this chapter we will justify this claim, and investigate potential control solutions. It should be noted right away that the simplest method for dealing with these factors is to try to reduce them directly with mechanical design, and that non of the control solutions below yield a perfect result.

5.1 Friction

Four different friction models is depicted in [(28) fig. 5.1], where friction model d) which includes the stribeck effect (29), is the most realistic of them. However, model c) which includes static friction is enough to reproduce most of the unwanted effects (30).

A mathematical model (29) of friction model c) is shown in equation (5.1). Where F_c is the Coulomb force, which is proportional to load. F_v is the proportionality constant of the linear viscous friction, F is the sum of forces from the outside action on the system, and F_s is the static friction force (also called stiction). The positive direction of F_f is defined opposite of the positive direction of F and v. When the system is motionless, the external forces has to overcome the static friction to *release* the system into motion. The stiction force is greater than the coulomb force, resulting in a drop in friction when the system is released.

$$F_f(v,F) = \begin{cases} F, & v = 0 \cap F_s > F \\ F_s sgn(F), & v = 0 \cap F_s \leq F \\ F_c sgn(v) + F_v \cdot v, & v \neq 0 \end{cases} \tag{5.1}$$

The friction model is discontinuous at v=0, and position or trajectory control of the robotic finger entails crossing this point frequently. While approaching the desired position, the system can enter a limit cycle called *hunting*, or *stick/slip-cycle* (31), where the system overshoots the target because of the torque required to break free from stiction, and therefore never settles. The stick/slip cycle keeps us from reaching the desired position, and reduces the accuracy of the position/tracking control system.

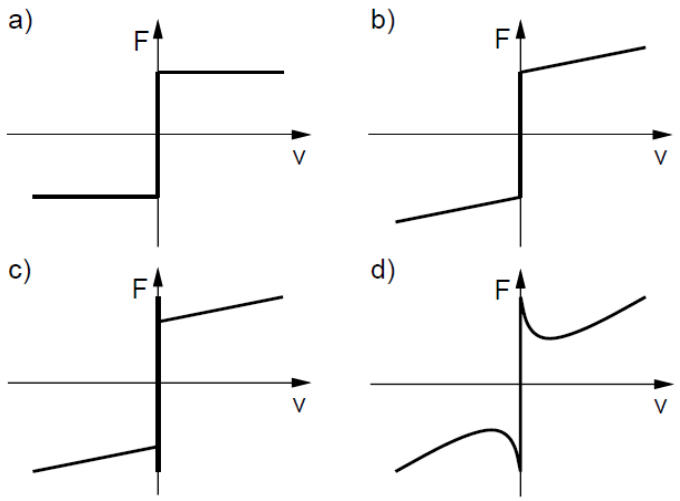

Figure 5.1: a) Coulomb model, b) Coulomb + viscosity, c) Coulomb + viscosity + static friction d) Coulomb + viscosity + stribeck effect

BrianArmstrong-Hélouvry, PierreDupont, Carlos CanudasDe Wit (1994) (30) provides a comprehensive survey of compansation methods for control of machines with friction. One of the results is that model a) (coloumb model) *does not* cause stick/slip cycles for PD or PID position control or PD tracking control, while a model with Coulomb + stiction *can* cause stick/slip cycles for PID position control, and PD and PID tracking control, but not with PD position control (30). This tells us that Coulomb friction and viscous friction are not important factors for accuracy, and that the integral gain must be adjusted carefully when controlling the position of systems with friction. The stribeck effect is the dominant *frictional contributer* in low speed tracking control, where it can cause stick-/slip cycles (30). Stiction is the dominant frictional contributor in tracking with velocity reversal where it can cause stops and lost motion (30), and is also the dominant frictional contributor in position control where it can cause steady state error with PD, and *hunting* (limit cycle around a point) with PID control (30). Viscous friction is the dominant frictional contributor in high velocity tracking, where it causes high tracking errors (30). However, this sets a limit on velocity rather than accuracy.

In the survey (30), several compensation methods were suggested specifically for robotics;

- Tracking with reversal
  - Coulomb Friction Feedforward/Feedback
  - General Friction Feedforward/Feedback
  - Adaptive Feedforward/Feedback
- Tracking with low velocity
  - Joint Torque control

  - Impulsive control / Dither

- Tracking with high velocity
  - Integral Control / Deadband
  - Joint Torque Control
  - Coulomb Friction Feedforward/Feedback
  - Adaptive Feedforward/Feedback

5.1.1 Integral control with deadband

To counteract the stick/slip cycles induced by integral action, a solution is to introduce a deadband as the input of of the integrator (30). During velocity reversal, integral windup can hinder the system in breaking away. This can be solved by resetting the integrator at velocity reversals (30). The deadband *does* cause steady state errors since the integrator essentially "stops trying" when the error is small enough.

5.1.2 Dither

Dither is the introduction of high frequency vibrations to the system to smooth out the discontinuous elements in friction. In tangential dither, a high frequency signal is supplied through the control signal (30). Simply put; the average contributions of tangential dither is zero, but it keeps the system close to-, or in a continuous state of "breaking away". Normal dither is vibrations introduced through the contract surface (30).

5.1.3 Impulsive control

Impulsive control use torque impulses when the system is at rest or at very low velocity. The magnitude or duration of the pulse can be used to calibrate the impact of the impulse in terms of movement (30).

5.1.4 Friction Feedforward/Feedback

Friction can be estimated, modeled, or collected in a look-up table to be used in feedforward or feedback to eliminate the unwanted effects (30).

5.1.5 Adaptive Feedforward/Feedback

Adaptive control react to changing or uncertain parameters by changing the control law itself (32). As an example, robots can utilize adaptive control to adjust the control law when picking up an object of unknown mass. In model reference adaptive control, the control law is changed based on the difference between the actual response and the wanted response (32). Model identification adaptive control tries to identify model parameters and adjust the control law accordingly (32). The concept is applicable to other uncertainties including friction.

5.1.6 Joint Torque control

Joint torque control utilizes a cascade control strategy with torque feedback which is measured as close to the output as possible (30). This is different from the reference model in figure 4.2 which uses current feedback. Since the torque measurements in joint torque control is measured after disturbances (in the extent that it is possible), the inner loop is able to compensate without help from the slower outer loop.

A related concept is acceleration feedback. Acceleration is proportional to the torque we are attempting to measure in joint torque control. The drawback is that acceleration has to be estimated. A method (33) which showed promising results used a velocity observer, and motor torque to feed a nonlinear friction estimator, which in turn was used to estimate acceleration.

5.2 Elasticity

The equations of motion of an undisturbed rigid system is shown in equation 5.2, and the equations of motion of an undisturbed elastic system (17) is shown in equation 5.3a-5.3b, where J_m and J_l is the motor and load inertia, B_m B_l is the motor and load damping constants, and u is the motor torque.

$$J_m\ddot{\theta}_m = B_m\dot{\theta}_l = u \tag{5.2}$$

$$J_l\ddot{\theta}_l = B_l\dot{\theta}_l + k(\theta_l - \theta_m) = 0 \tag{5.3a}$$

$$J_m\ddot{\theta}_m = B_m\dot{\theta}_m + k(\theta_l - \theta_m) = u \tag{5.3b}$$

The addition of elasticity doubled the number of states, and the model is now a fourth order single input single output system (SISO). If the load friction coefficient B_l is small (which is often the case), the system becomes very hard to control (17). Using only one state as feedback for position control (motor angle or load angle), a PD controller can achieve a critically damped step response for motor angle *or* load angle, but not both (17). In fact, with load angle feedback, the load angle response will either be oscillatory, very slow, or both (or unstable) (17). However, the load angle is the control objective, so we need a way to utilize it if the system is sufficiently elastic.

One solution to this problem is to use state feedback. Since the system is controllable, we can theoretically place the poles wherever we want as long as they come in complex conjugate pairs (17). In practice there are limitations. The bandwidth must be sufficiently low to achieve bandwidth separation from both the torque control loop, and any potential observers.

5.3 Backlash

Backlash is the gap the driver axle can travel without any mechanical output on the driven axle. It is caused by the spaces in between parts, and can be modeled as a hysteresis.

Backlash can cause the load to oscillate because of low damping in the dead-zone (29). However, by tracking the position on both axles, velocity in the dead-zone can be observed, and damping can be introduced as a control law to make the system stable (29). Alternatively, the gears can be spring loaded to "stick together" on one side (34). Another solution is to use an offset torque in the opposite direction of rotation (29).

Chapter 6

Choosing a suitable reduction gearbox

A rough approximation of the reduction ratio has already been decided in chapter 3.2. The choice of transmission system will therefore be based on friction, elasticity and backlash, price, weight and size.

In chapter 5.1 we found that static friction was the dominant frictional contributor to our control system. However, commercially available gears are rated in terms of efficiency at rated speed, which has nothing to do with stiction. This makes comparisons difficult without acquiring gears for testing. Since efficiency is all we have, we will use it when comparing systems.

An overview of the pros and cons of 3 common transmission systems is shown in [(35) fig. 6.1]. Spur gears are generally cheap, but are not ideal because of the backlash. Toothed belts are elastic, but has no backlash. Impact loads can potentially cause the belt to slip, which can be problematic for position control. Out of the three options, planetary gears seems like the best choice because of high efficiency and low backlash.

Strain wave gears are a popular choice in robotics because they have no backlash (17), offer extremely high single stage gear ratio and is therefore very compact (36). They do however have non-negligible elasticity (17), and they are expensive (36). As stated

Type	Efficiency	Pros	Cons
Spur	High	Parallel shafting. High speeds and loads.	Can have back backlash, especially at low speeds or in a reversible situation. Low flexibility in input and output shaft configuration. Needs lubrication.
Planetary	High	Very low backlash. Compact size and low weight. Low maintenance. Fully reversible.	More complex design. Higher cost than simple spur gearheads. Low flexibility in input and output shaft configuration. Needs lubrication.
Toothed Belts	Medium	Smoother running. Flexibility in arrangement of input and output shafts. Require no lubrication.	Elastic play is high. Sensitive to impact loads. Must be tensioned (resulting radial forces must be absorbed through design). Open to electrostatic charges.

Figure 6.1: Pros and cons of 3 common transmission systems

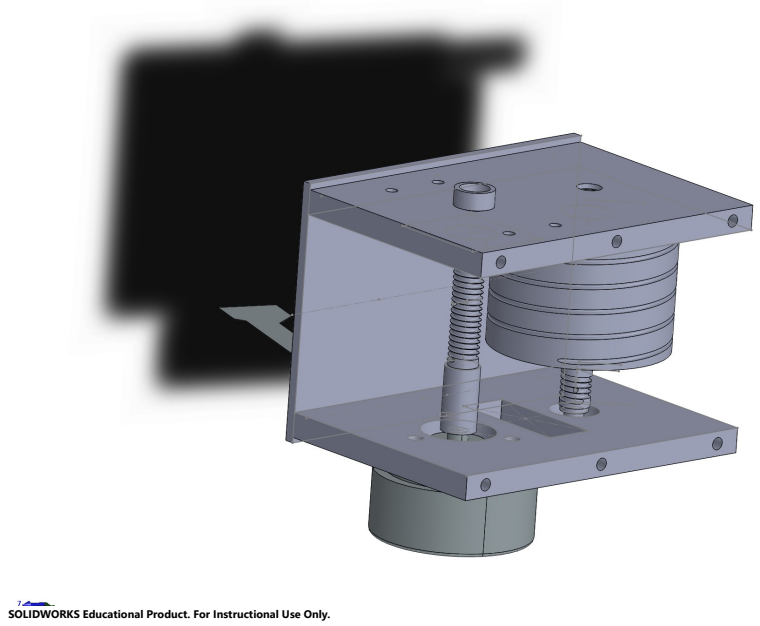

Figure 6.2: 3D view of the custom transmission system

earlier; high reduction ratios reduces the back driving capability. Thus, for this project, strain wave systems are essentially no more useful than a toothed belt system.

6.1 Custom transmission system based on pulleys

In the pursuit of a transmission system with extremely low friction, elasticity and backlash, a custom transmission system based on pulleys was designed. A 3D view of the system is shown in figure 6.2, and the concept is illustrated in figure 6.3.

The motor is connected to the left spindle, which drives the second spindle with a string resulting in a reduction ratio of 6. At the bottom of the right axle, there is a low radius spindle which drives the tendons connected to the finger joint (1). This last connection represents the second stage in the reduction gear with a reduction ratio of 5, which makes the total reduction ratio 30. On top of the gearbox, there is a small cup which rotates with the drive spindle. The cup is intended to hold a magnet used for position sensing of the motor axle.

The transmission system is still under construction at the mechanical workshop at Gløshaugen NTNU, but is almost done. Blueprints for the system can be found in appendix C.

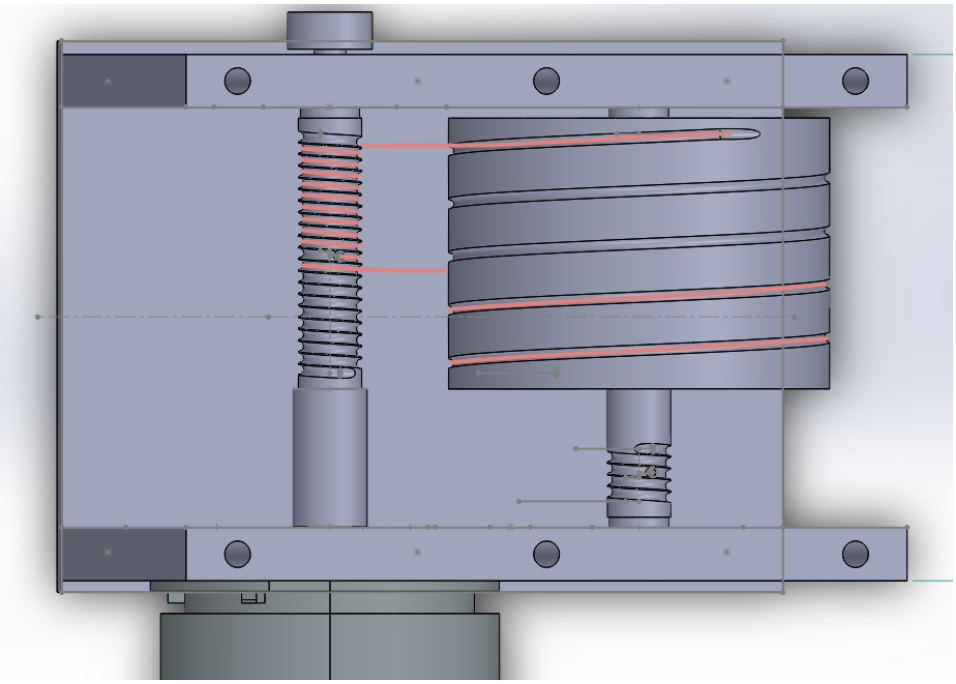

Figure 6.3: Illustration of how the custom transmission system works

6.1.1 Design philosophy

The elasticity of the system is entirely dependant on the elasticity of the string, which gives room for experimentation with many different materials. While a toothed belt system is tightened so that it wont slip when loaded, this system is tightened to reduce backlash. This could potentially mean less required tension, lower load on the bearings, and in turn; less friction. Instead of friction from the "teeth" of a toothed belt sliding into place, we get friction from the string sliding in place into the groove. Hopefully, this causes very little friction.

Downsides: Large size and weight (18x70x52mm and 0.17Kg without motor), but there is room for improvements. Both weight and size can be reduced if a lower reduction ratio is used. Two gear systems will share the same chassis and save space and weight. The large spindle can also be made partially hollow to reduce weight. Custom made parts are not cheap or "of the shelf", but the system should be easy to repair.

6.1.2 Similar concepts

Towards the end of this project i was made aware of a similar project (37). Unfortunately, "low friction" was not mentioned as a key design feature. However, the system did have zero backlash. The system did also have back driving capability, in the sense that tendons are configured so that movement of fingers results in movement of the motor. Elasticity was purposely introduced in the design to tighten the tendons. This is the opposite of our approach. They did not use grooves to position the wires. Since the wires are spring loaded, running the motor back and fourth a few times produced a stable configuration.

6.2 Gear choice

The custom transmission system seems promising for now, and will be ready for testing in early January. If the advantages (if any), does not outweigh the disadvantages (weight, size, custom build), a planetary gear will be used instead.

Chapter 7

Conclusion and future work

7.1 Conclusion

The chosen actuator system is a 15W BLDC-motor with a custom made reduction gear. The chosen low level control system is a PI torque controller with current feedback, trapezoidal commutation controlled with hall sensor feedback. The system is untested, but potential problems and solutions to them has been identified

System specifications

- Total weight: 0.23 Kg
- Nominal torque: 0.765 Nm
- Nominal speed: 92 rpm
- Supply voltage: 24V
- Nominal current: 0.5A
- Output power: 15W
- Controller type: PI, current feedback, Hall sensor based trapezoidal commutation
- Controller sampling rate: 53.6 kHz
- Pulse width modulation frequency 53.6 kHz

7.2 Future work

To complete the work of choosing a suitable actuator and low level control system for a dexterous manipulator, the custom made reduction gear will have to be tested and compared with a planetary gear to confirm any advantages. The controller will also have to be tested to find out whether or not the torque ripple inherent to trapezoidal commutation

causes jittery movement, and if special control strategies is needed because of friction, elasticity or backlash.

Bibliography

[1] A. Danielsen, "Konstruksjon av finger til avansert robot hand," 2018.

[2] "Gelsight." [Online]. Available: http://www.gelsight.com/

[3] A. M. Okamura, N. Smaby, and M. R. Cutkosky, "An overview of dexterous manipulation," in *Proceedings 2000 ICRA. Millennium Conference. IEEE International Conference on Robotics and Automation. Symposia Proceedings (Cat. No.00CH37065)*, vol. 1, April 2000, pp. 255–262 vol.1.

[4] "what is an actuator?" 2018. [Online]. Available: https://www.techopedia.com/definition/17043/actuator

[5] "Artificial muscle," 2018. [Online]. Available: https://en.wikipedia.org/wiki/Artificial_muscle

[6] J. M. Hollerbach, I. W. Hunter, and J. Ballantyne, "The robotics review 2," O. Khatib, J. J. Craig, and T. Lozano-Pérez, Eds. Cambridge, MA, USA: MIT Press, 1992, ch. A Comparative Analysis of Actuator Technologies for Robotics, pp. 299–342. [Online]. Available: http://dl.acm.org/citation.cfm?id=146312.146323

[7] C. Gonzalez, "What's the difference between pneumatic, hydraulic, and electrical actuators?" 2015. [Online]. Available: https://www.machinedesign.com/linear-motion/what-s-difference-between-pneumatic-hydraulic-and-electrical-actuators

[8] "Pneumatics," Dec 2018. [Online]. Available: https://en.wikipedia.org/wiki/Pneumatics

[9] S. Rosenfeld, "Advantages and drawbacks of pneumatic, hydraulic, and electric linear actuators," 2017. [Online]. Available: https://www.timotion.com/cn/news/news_content/blog-articles/general/advantages-and-drawbacks-of-pneumatic,-hydraulic,-and-electric-linear-actuators?upcls=1481266229&guid=1499762723

[10] Y. Honda, F. Miyazaki, and A. Nishikawa, "Control of pneumatic five-fingered robot hand using antagonistic muscle ratio and antagonistic muscle activity," in *2010 3rd IEEE RAS EMBS International Conference on Biomedical Robotics and Biomechatronics*, Sep. 2010, pp. 337–342.

[11] T. Kang, H. Kaminaga, and Y. Nakamura, "A robot hand driven by hydraulic cluster actuators," in *2014 IEEE-RAS International Conference on Humanoid Robots*, Nov 2014, pp. 39–44.

[12] H. Kaminaga, J. Ono, Y. Nakashima, and Y. Nakamura, "Development of backdrivable hydraulic joint mechanism for knee joint of humanoid robots," in *2009 IEEE International Conference on Robotics and Automation*, May 2009, pp. 1577–1582.

[13] N. S. Pollard and R. C. Gilbert, "Tendon arrangement and muscle force requirements for human-like force capabilities in a robotic finger," in *Proceedings 2002 IEEE International Conference on Robotics and Automation (Cat. No.02CH37292)*, vol. 4, May 2002, pp. 3755–3762 vol.4.

[14] "choosing a motor and gearing combination," 2018. [Online]. Available: http://hades.mech.northwestern.edu/index.php/Choosing_a_Motor_and_Gearing_Combination?fbclid=IwAR2WtsRQLMZg3vzHiGUpg-5ZWVIQ4LWG5HSCfcduVP8K-s4VIoie0WbhdmI

[15] T. Nef and P. Lum, "Improving backdrivability in geared rehabilitation robots," *Medical biological engineering computing*, vol. 47, pp. 441–7, 02 2009.

[16] [Online]. Available: https://www.maxonmotor.com

[17] M. Spong, S. Hutchinson, and M. Vidyasagar, *Robot Modeling and Control*, ser. Wiley select coursepack. Wiley, 2005. [Online]. Available: https://books.google.no/books?id=muCMAAAACAAJ

[18] R. Beard and T. McLain, *Small Unmanned Aircraft: Theory and Practice*. Princeton University Press, 2012. [Online]. Available: https://books.google.no/books?id=YqQtjhPUaNEC

[19] "Ziegler–nichols method," 2018. [Online]. Available: https://en.wikipedia.org/wiki/Ziegler\OT1\textendashNichols_method

[20] "Brushless dc motor," 2018. [Online]. Available: https://www.allaboutcircuits.com/textbook/alternating-current/chpt-13/brushless-dc-motor/

[21] ChamChin-Long and S. Bin, "Brushless dc motor electromagnetic torque estimation with single-phase current sensing," *Journal of Electrical Engineering and Technology*, vol. 9, no. 3, pp. 866–872.

[22] S. Keeping, "controlling sensorless bldc motors via back emf."

[23] Y. Liu, Z. Q. Zhu, and D. Howe, "Commutation-torque-ripple minimization in direct-torque-controlled pm brushless dc drives," *IEEE Transactions on Industry Applications*, vol. 43, no. 4, pp. 1012–1021, July 2007.

[24] D. Collins, "Faq: What is sinusoidal commutation for dc motors?" 2018. [Online]. Available: https://www.motioncontroltips.com/what-is-sinusoidal-commutation-for-dc-motors/

[25] “Implementing field oriented control of a brushless dc motor,” 2018. [Online]. Available: https://www.eetimes.com/document.asp?doc_id=1279321

[26] “Develop field-oriented control algorithms using simulation,” 2018. [Online]. Available: https://se.mathworks.com/discovery/field-oriented-control.html

[27] maxon motor ag, “maxon ec motor an introduction to brushless dc motors,” 2012. [Online]. Available: https://www.maxonmotor.com/medias/sys_master/root/8803450814494/maxonECmotor-Handouts.pdf?attachment=true

[28] “Why is the equation for friction so simple?” 2018. [Online]. Available: https://physics.stackexchange.com/questions/154443/why-is-the-equation-for-friction-so-simple

[29] O. Egeland and J. Gravdahl, *Modeling and Simulation for Automatic Control*, 01 2002.

[30] B. Armstrong-Hélouvry, P. Dupont, and C. Canudas De Wit, “A survey of models, analysis tools and compensation methods for the control of machines with friction,” *Automatica*, vol. 30, pp. 1083–1138, 07 1994.

[31] B. Armstrong-Helouvry, “Stick slip and control in low-speed motion,” *IEEE Transactions on Automatic Control*, vol. 38, no. 10, pp. 1483–1496, Oct 1993.

[32] “Adaptive control,” 2018. [Online]. Available: https://en.wikipedia.org/wiki/Adaptive_control

[33] Z. Wang, M. Zeng, and B. Su, “Friction compensation via acceleration feedback control based on friction estimation,” in *2006 International Conference on Machine Learning and Cybernetics*, Aug 2006, pp. 972–977.

[34] S. J. O’Neil, “Methods to minimize gear backlash,” 2018. [Online]. Available: https://www.machinedesign.com/motion-control/methods-minimize-gear-backlash

[35] “Choosing the right drive technology,” 2018. [Online]. Available: https://www.maxonmotorusa.com/medias/sys_master/root/8803697098782/Choosing-the-Right-Drive-Technology.pdf?attachment=true

[36] “the me guide to gears,” 2018. [Online]. Available: https://www.maintenanceandengineering.com/2018/04/06/the-me-guide-to-gears/?fbclid=IwAR27EIFEzReTuz0gWDT_Es4WXIzkldYICwTih2ywcoYYtuZ7pd9JhiPtuWM

[37] R. B. Hellman and V. J. Santos, “Design of a back-driveable actuation system for modular control of tendon-driven robot hands,” in *2012 4th IEEE RAS EMBS International Conference on Biomedical Robotics and Biomechatronics (BioRob)*, June 2012, pp. 1293–1298.

Appendix A

Datasheet for BLDC motor

EC 32 flat ∅32 mm, brushless, 15 Watt

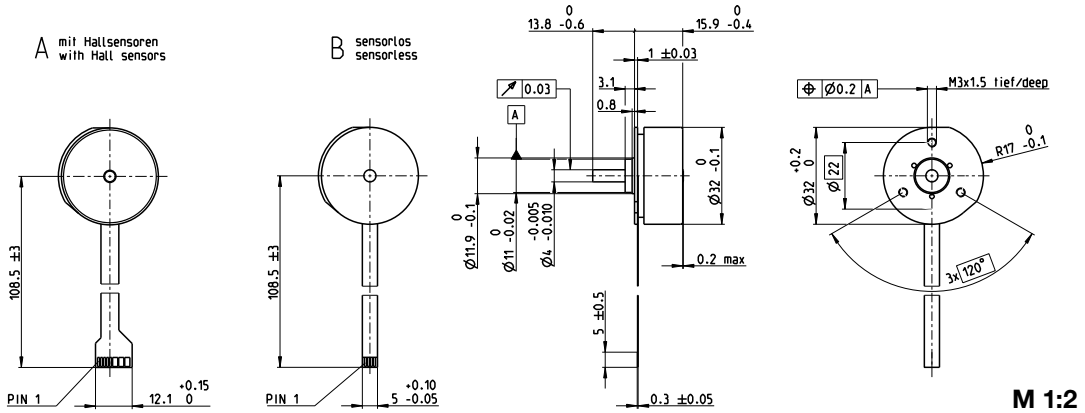

M 1:2

Stock program
Standard program
Special program (on request)

Part Numbers

A with Hall sensors	339267	339268	**267121**	339269
B sensorless	339271	339272	226006	339273

Motor Data

	Values at nominal voltage					
1	Nominal voltage	V	9	12	24	48
2	No load speed	rpm	3720	4610	4530	4780
3	No load current	mA	74.7	75.7	36.9	19.9
4	Nominal speed	rpm	2060	2790	2760	2940
5	Nominal torque (max. continuous torque)	mNm	24.5	25	25.5	24.7
6	Nominal current (max. continuous current)	A	1.06	1	0.5	0.257
7	Stall torque[1]	mNm	68.3	82.3	85.3	83.9
8	Stall current	A	3.06	3.42	1.74	0.904
9	Max. efficiency	%	71	73	73	73
	Characteristics					
10	Terminal resistance phase to phase	Ω	2.95	3.51	13.8	53.1
11	Terminal inductance phase to phase	mH	1.61	1.86	7.72	27.7
12	Torque constant	mNm/A	22.4	24.1	49	92.8
13	Speed constant	rpm/V	427	397	195	103
14	Speed/torque gradient	rpm/mNm	56.3	57.8	54.8	58.8
15	Mechanical time constant	ms	20.6	21.2	20.1	21.6
16	Rotor inertia	gcm²	35	35	35	35

Specifications

	Thermal data	
17	Thermal resistance housing-ambient	10.8 K/W
18	Thermal resistance winding-housing	4.99 K/W
19	Thermal time constant winding	8.78 s
20	Thermal time constant motor	120 s
21	Ambient temperature	-40…+100°C
22	Max. winding temperature	+125°C
	Mechanical data (preloaded ball bearings)	
23	Max. speed	10000 rpm
24	Axial play at axial load < 5.0 N	0 mm
	> 5.0 N	typ. 0.6 mm
25	Radial play	preloaded
26	Max. axial load (dynamic)	4.8 N
27	Max. force for press fits (static)	45 N
	(static, shaft supported)	1000 N
28	Max. radial load, 5 mm from flange	14 N
	Other specifications	
29	Number of pole pairs	4
30	Number of phases	3
31	Weight of motor	57 g

Values listed in the table are nominal.

Connection	**with Hall sensors**	**sensorless**
Pin 1	V_{Hall} 3.5…24 VDC	Motor winding 1
Pin 2	Hall sensor 3	Motor winding 2
Pin 3	Hall sensor 1	Motor winding 3
Pin 4	Hall sensor 2	⅄ neutral point
Pin 5	GND	
Pin 6	Motor winding 3	
Pin 7	Motor winding 2	
Pin 8	Motor winding 1	
Adapter	**Part number**	**Part number**
see p. 471	220300	220310
Connector	**Part number**	**Part number**
Tyco	1-84953-1	84953-4
Molex	52207-1133	52207-0433
Molex	52089-1119	52089-0419

Pin for design with Hall sensors:
FPC, 11-pol, Pitch 1.0 mm, top contact style
Wiring diagram for Hall sensors see p. 43
[1]Calculation does not include saturation effect (p. 53/164)

Operating Range

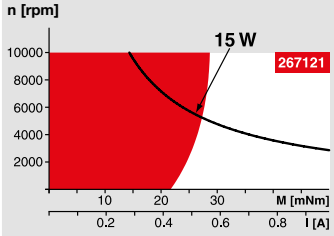

Comments

Continuous operation
In observation of above listed thermal resistance (lines 17 and 18) the maximum permissible winding temperature will be reached during continuous operation at 25°C ambient.
= Thermal limit.

Short term operation
The motor may be briefly overloaded (recurring).

Assigned power rating

maxon Modular System

Overview on page 28–36

Planetary Gearhead
∅32 mm
0.75 - 6 Nm
Page 344/347

Spur Gearhead
∅38 mm
0.1 - 0.6 Nm
Page 353

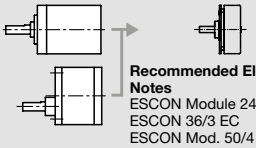

Recommended Electronics:

Notes	**Page 32**
ESCON Module 24/2	444
ESCON 36/3 EC	445
ESCON Mod. 50/4 EC-S	445
ESCON Module 50/5	445
ESCON 50/5	447
DEC Module 24/2	449
DEC Module 50/5	449
EPOS4 Mod./Comp. 24/1.5	452
EPOS4 50/5	453
EPOS4 Mod./Comp. 50/5	453
MAXPOS 50/5	468

Appendix B

Datasheet for PI torque controller (Trapezoidal commutation)

ESCON Overview

The ESCON servo controllers are small-sized, powerful 4-quadrant PWM servo controller for the highly efficient control of permanent magnet-activated DC motors.

The featured operating modes – speed control (closed loop), speed control (open loop), and current control – meet the highest requirements. The ESCON servo controllers are designed being commanded by an analog set value and features extensive analog and digital I/O functionality and are being configured via USB interface using the graphical user interface "ESCON Studio" for Windows PCs.

ESCON Module 24/2
466023

ESCON 36/2 DC
403112

ESCON 36/3 EC
414533

ESCON Module 50/4 EC-S
446925

ESCON Module 50/5
438725

ESCON 50/5
409510

ESCON Module 50/8 (HE)
532872
586137

ESCON 70/10
422969

Depending on the ESCON variant, the following **motor types** can be operated
- **DC motor:** Permanent-magnet DC motor
- **EC motor:** Brushless, electronically commutated permanent-magnet DC motor (BLDC) with and without Hall sensors.

Various **operating modes** allow an adaptable use in a wide range of drive systems
- **Current controller:** The current controller compares the actual motor current (torque) with the applied set value. In case of deviation, the motor current is dynamically readjusted.
- **Speed controller (closed loop):** The closed loop speed controller compares the actual speed signal with the applied set value. In case of deviation, the speed is dynamically readjusted.
- **Speed controller (open loop):** The open loop speed controller feeds the motor with a voltage proportional to the applied speed set value. Changes in load are compensated using the IxR methodology.

Speed measurement by
- **Digital incremental encoder:** The encoders deliver simple square signals for further processing. Their impulses are counted to determine the speed. Channels A and B are phase-shifted signals, which are being compared to determine the direction of rotation.
- **DC tacho:** The DC tacho delivers a speed-proportional analog voltage.
- **Available Hall sensors:** The Hall sensors deliver six different combinations of switching impulses per electrical turn which are counted to determine speed. They also deliver phase-shifted signals that are being compared to determine the direction of rotation.
- **Sensorless EC:** The speed is determined by the progression of the induced voltage. The electronics evaluates the zero crossing of the induced voltage (EMF).

To the numerous **inputs** and **outputs,** various functionalities can be assigned to.

Set value (speed or current), **current limitation,** as well as **offset** can be assigned as follows.
- **Analog value:** The value is defined by an analog voltage set via external or internal potentiometer.
- **PWM value:** The value is defined by fixed frequency and amplitude. The desired change is achieved by variation of the duty cycle of 10…90%.
- **RC Servo Value:** The value is set with a signal pulse with a duration of 1.0…2.0 ms.
- **Fixed value:** The value is defined by a fixed preset value.
- **2 fixed values:** Value 1 is defined by a fixed preset value 1. Value 2 is defined by a fixed preset value 2. A digital input is used to switch between the two preset values.

Various functionalities are available to **enable** the power stage.
- **Enable:** Enables or disables the power stage.
- **Enable & Direction:** Enables or disables the power stage and determines the motor shaft's direction of rotation.

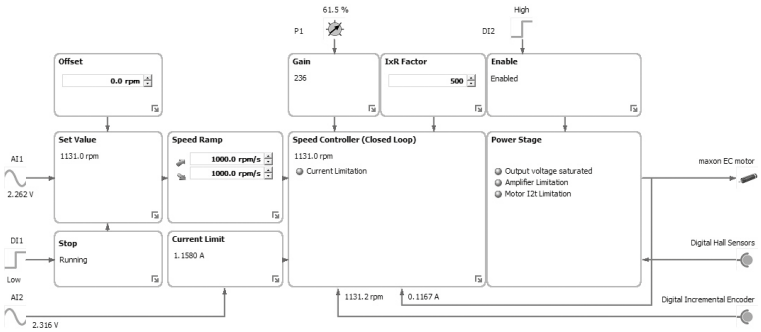

ESCON Studio (Controller Monitor)

Software
Installation Program: ESCON Setup
Graphical User Interface: ESCON Studio
✓ Startup Wizard
✓ Regulation Tuning
✓ Diagnostic
✓ Firmware Update
✓ Controller Monitor
✓ Parameters
✓ Data Recording
✓ Online Help
Language: German, English, French, Italian, Spanish, Japanese, Chinese
Operating System: Windows 10, Windows 8, Windows 7, Windows XP SP3
Communication interface: USB 2.0/3.0 (full speed)

– **Enable CW:** Enables or disables the power stage in direction of rotation-dependent sense. The rotor can only turn clockwise (CW).
– **Enable CCW:** Enables or disables the power stage in direction of rotation-dependent sense. The rotor can only turn counterclockwise (CCW).
– **Enable CW & CCW:** Enables or disables the power stage in direction of rotation-dependent sense. The rotor can only turn in defined direction. The signals are interlocked against each other.

The **ramp function** permits controlled acceleration/deceleration of the motor shaft in both, open loop and closed loop speed controller mode.
– **Analog ramp:** The ramp is defined by a variable analog value.
– **Fixed ramp:** The ramp is defined by a fixed preset value.

Stop: The motor shaft decelerates with preset speed ramp until complete standstill.

Ready: The Ready signal can be used to transmit the operational status (respectively fault) to a superior control.

Speed and Current Comparator: The digital output is set depending on the actual value.
– **Limit:** The digital output is set as soon as the preset value is reached. It remains set as long as the value is exceeded.
– **Range:** The digital output is set as soon as the preset value range is reached. It remains set as long as the value remains in range.
– **Deviation:** The digital output is set as soon as the preset value deviation (based on the set value) is in range.

With the integrated **potentiometers** the additional following functions can be adjusted
– **Current Gain:** Adjustment of the current controller gain.
– **Speed Gain:** Adjustment of the speed controller gain.
– **IxR Factor:** The voltage drop caused by terminal resistance will be compensated in the range of [0…1000…2000].

Analog outputs allow monitoring of
– **Actual current:** Actually measured motor winding current.
– **Actual current averaged:** Actually measured motor winding current filtered by first order digital low-pass filter with a cut-off frequency of 5 Hz.

Easy startup
Startup and parameterization are performed using the intuitive graphical user interface “ESCON Studio” with the help of simple to use, menu-guided wizards. The following wizards are available: Startup, Regulation Tuning, Firmware Update, Controller Monitor, Parameters, Data Recording, and Diagnostics.

Protective equipment
The servo controller has protective circuits against overcurrent, excess temperature, under- and overvoltage, against voltage transients, and against short-circuits in the motor cable. Furthermore it is equipped with protected digital inputs and outputs and an adjustable current limitation for protecting the motor and the load. The motor current and the actual speed of the motor shaft can be monitored by means of the analog output voltage.

Comprehensive documentation
Using the “Feature Comparison Chart”, the suitable ESCON servo controller can easily be determined. The “Hardware Reference” comprises the specifications of the hardware in detail. The documents “Firmware Version” and “Release Notes” describe changes and improvements of firmware and software. In addition, the graphical user interface “ESCON Studio” features a comprehensive online help.

– **Actual speed:** Actually measured motor speed.
– **Actual speed averaged:** Actually measured motor speed filtered by 1st order digital low-pass filter with a cut-off frequency of 5 Hz.
– **Demand Current:** Demanded motor winding current.
– **Demand Speed:** Demanded motor speed.
– **Temperature Power Stage:** Actually measured power stage temperature.
– **Fixed value:** The output voltage is said fixed to the preset value.

Accessories ESCON (not included in delivery)	Module 24/2	36/2 DC	36/3 EC	Module 50/4 EC-S	Module 50/5	50/5	Module 50/8	Module 50/8 HE	70/10
404404 ESCON 36/2 DC Connector Set	–	✓	–	–	–	–	–	–	–
425255 ESCON 36/3 EC Connector Set	–	–	✓	–	–	–	–	–	–
403962 DC Motor Cable	–	✓	–	–	–	–	–	–	–
403964 I/O Cable 7core (analog I/O’s)	–	✓	✓	–	–	–	–	–	–
403965 I/O Cable 6core (digital I/O’s)	–	✓	✓	–	–	–	–	–	–
275934 Encoder Cable	–	✓	–	–	–	✓	–	–	✓
403957 Power Cable	–	✓	✓	–	–	–	–	–	–
403968 USB Type A - micro B Cable	✓	✓	✓	✓	✓	✓	✓	✓	✓
418719 Adapter BLACK FPC11poles	–	–	✓	–	–	–	–	–	–
418723 Adapter BLUE FPC8poles	–	–	✓	–	–	–	–	–	–
418721 Adapter GREEN FPC8poles	–	–	✓	–	–	–	–	–	–
486400 ESCON Module 24/2 Motherboard	✓	–	–	–	–	–	–	–	–
438779 ESCON Module Motherboard	–	–	–	–	✓	–	–	–	–
586048 ESCON Module 50/8 Motherboard	–	–	–	–	–	–	✓	✓	–
450237 ESCON Module Motherboard Sensorless	–	–	–	✓	–	–	–	–	–
409286 ESCON USB Stick	✓	✓	✓	✓	✓	✓	✓	✓	✓
586142 ESCON Module 50/8 Thermal Pad	–	–	–	–	–	–	✓	–	–

ESCON Feature Comparison Chart

	ESCON Module 24/2	ESCON 36/2 DC
DC motors up to (continuous / maximum)	48 W / 144 W	72 W / 144 W
EC motors up to (continuous / maximum)	48 W / 144 W	–
Sensors		
	Digital Incremental Encoder (2 channel with or without Line Driver)	Digital Incremental Encoder (2 channel with or without Line Driver)
	DC Tacho	DC Tacho
	Without sensor (DC motors)	Without sensor (DC motors)
	Digital Hall Sensors (EC motors)	–
Operating mode		
	Current controller (torque control), Speed controller (closed and open loop)	Current controller (torque control), Speed controller (closed and open loop)
Electrical data		
Nominal operating voltage V_{CC}	10 - 24 VDC	10 - 36 VDC
Max. output voltage	0.98 x V_{CC}	0.98 x V_{CC}
Max. output current	6 A (<4 s)	4 A (<60 s)
Continuous output current	2 A	2 A
Pulse width modulation frequency	53.6 kHz	53.6 kHz
Sampling rate PI current controller	53.6 kHz	53.6 kHz
Sampling rate PI speed controller	5.36 kHz	5.36 kHz
Max. efficiency	92%	95%
Max. speed (DC)	limited by max. speed (motor) and max. output voltage (controller)	limited by max. speed (motor) and max. output voltage (controller)
Max. speed (EC; 1 pole pair)	150000 rpm	–
Built-in motor choke	–	300 µH / 2 A
Inputs/Outputs		
Hall sensor signals	H1, H2, H3	–
Encoder signals	A, A\, B, B\	A, A\, B, B\
Max. encoder input frequency differential (single-ended)	1 MHz (100 kHz)	1 MHz (100 kHz)
Potentiometers	–	1
Digital inputs	2	2
Digital inputs/outputs	2	2
Analog inputs Resolution, Range, Circuit	2 12-bit, -10…+10 V, differential	2 12-bit, -10…+10 V, differential
Analog outputs Resolution, Range, Max. output current	2 12-bit, -4…+4 V, 1 mA	2 12-bit, -4…+4 V, 1 mA
Auxiliary voltage output	+5 VDC (IL ≤10 mA)	+5 VDC (IL ≤10 mA)
Hall sensor supply voltage	+5 VDC (IL ≤30 mA)	–
Encoder supply voltage	+5 VDC (IL ≤70 mA)	+5 VDC (IL ≤70 mA)
Status Indicators	Operation: green LED / Error: red LED	Operation: green LED / Error: red LED
Environmental conditions		
Temperature – Operation	-30…+60°C	-30…+45°C
Temperature – Extended range	+60…+80°C; Derating: -0.100 A/°C	+45…+81°C; Derating: -0.056 A/°C
Temperature – Storage	-40…+85°C	-40…+85°C
Humidity (condensation not permitted)	5…90%	5…90%
Mechanical data		
Weight	Approx. 7 g	Approx. 30 g
Dimensions (L x W x H)	35.6 x 26.7 x 12.7 mm	55.0 x 40.0 x 16.1 mm
Mounting holes	Plugable (socket headers with 2.54 mm pitch)	for screws M2.5
Part numbers		
	466023 ESCON Module 24/2	**403112** ESCON 36/2 DC
	Order accessories separately, from page 470	Order accessories separately, from page 470

Appendix C

Blueprints for custom transmission system

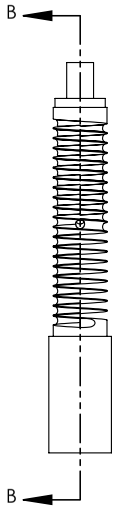

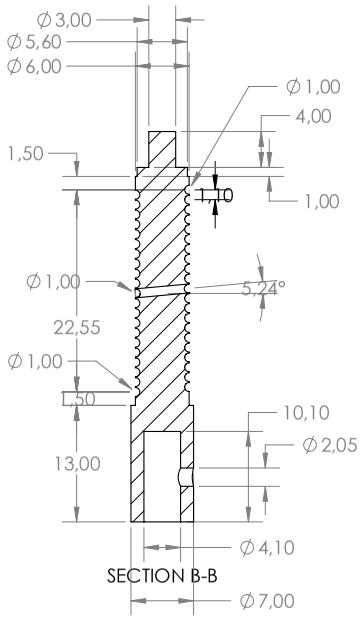

SECTION B-B

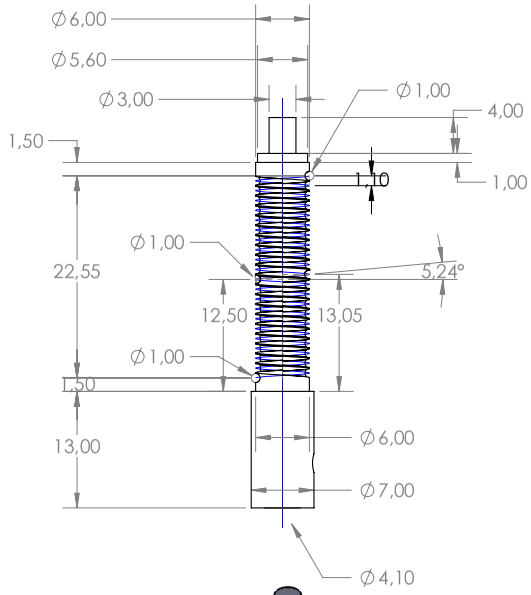

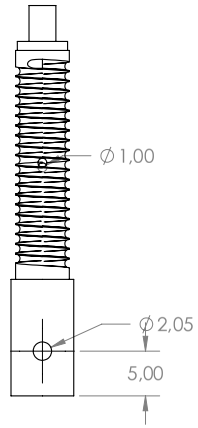

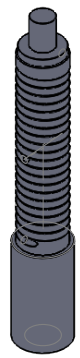

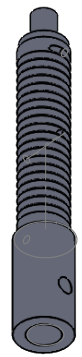

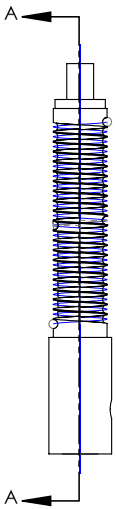

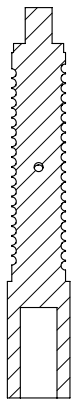

SECTION A-A

UNLESS OTHERWISE SPECIFIED: DIMENSIONS ARE IN MILLIMETERS SURFACE FINISH: TOLERANCES: LINEAR: ANGULAR:		FINISH:			DEBURR AND BREAK SHARP EDGES	DO NOT SCALE DRAWING	REVISION
	NAME	SIGNATURE	DATE			TITLE:	
DRAWN							
CHK'D							
APPV'D							
MFG							
Q.A				MATERIAL:		DWG NO. motorspole1	A3
				WEIGHT:		SCALE:2:1	SHEET 1 OF 1

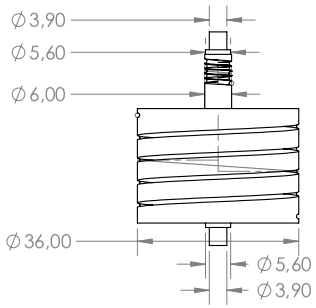

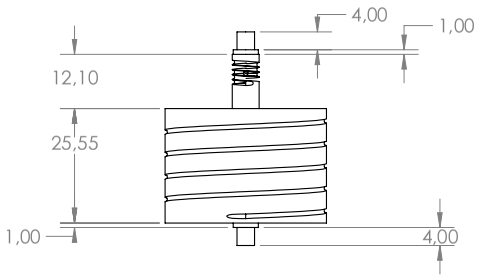

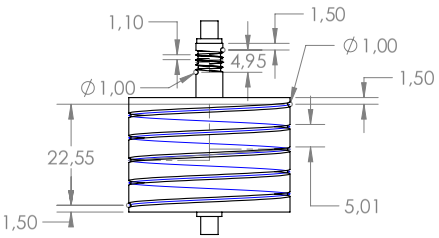

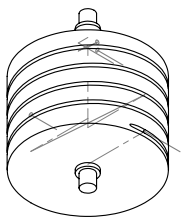

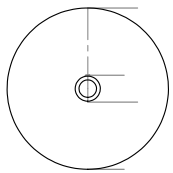

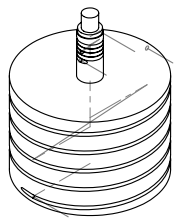

UNLESS OTHERWISE SPECIFIED: DIMENSIONS ARE IN MILLIMETERS SURFACE FINISH: TOLERANCES: LINEAR: ANGULAR:		FINISH:			DEBURR AND BREAK SHARP EDGES	DO NOT SCALE DRAWING	REVISION
	NAME	SIGNATURE	DATE			TITLE:	
DRAWN							
CHK'D							
APPV'D							
MFG							
Q.A				MATERIAL:		DWG NO. stor spole	A3
				WEIGHT:		SCALE:1:1	SHEET 1 OF 1

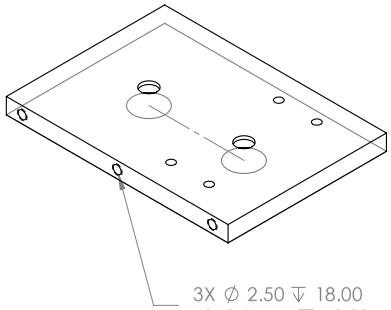

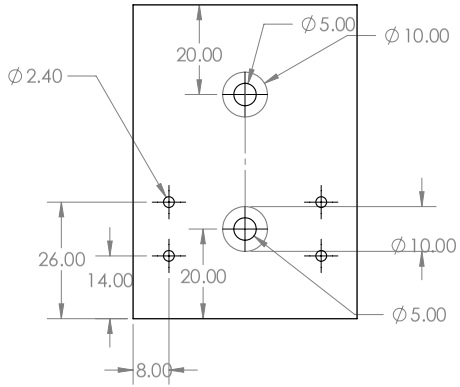

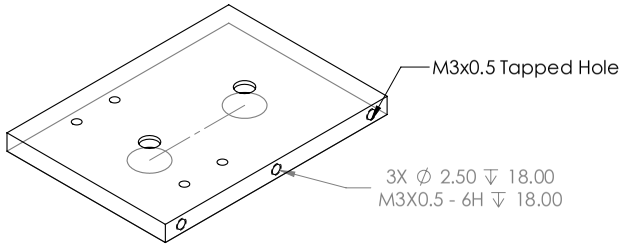

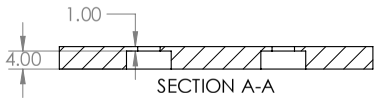

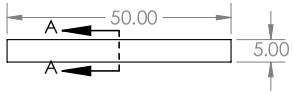

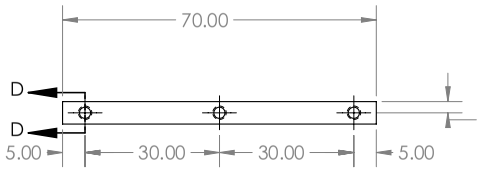

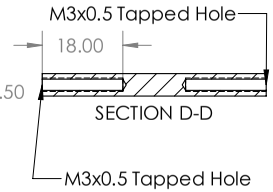

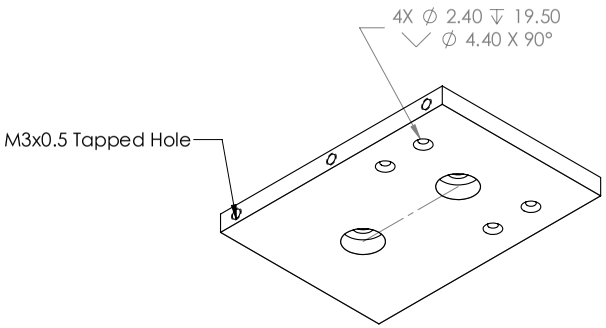

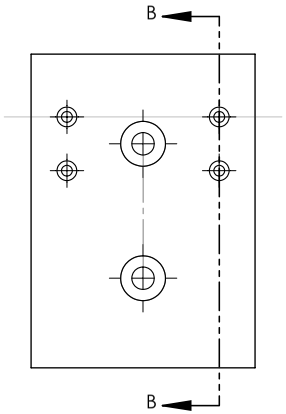

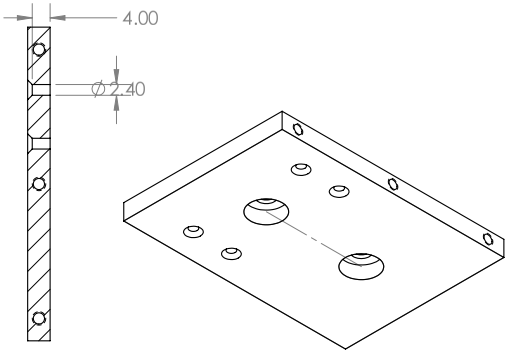

SECTION B-B

UNLESS OTHERWISE SPECIFIED: DIMENSIONS ARE IN MILLIMETERS SURFACE FINISH: TOLERANCES: LINEAR: ANGULAR:		FINISH:			DEBURR AND BREAK SHARP EDGES		DO NOT SCALE DRAWING	REVISION
	NAME	SIGNATURE	DATE				TITLE:	
DRAWN								
CHK'D								
APPV'D								
MFG								
Q.A				MATERIAL:			DWG NO. plate bunn	A3
				WEIGHT:			SCALE:1:1	SHEET 1 OF 1

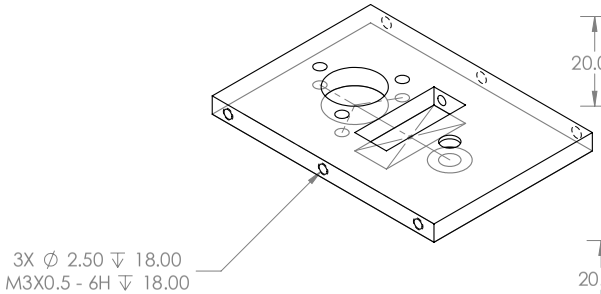

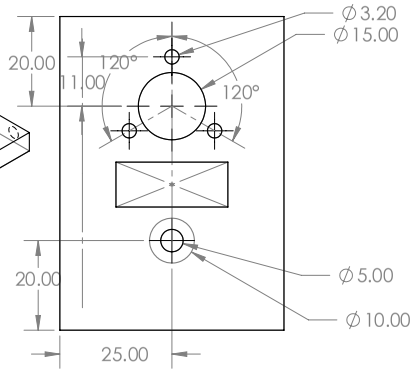

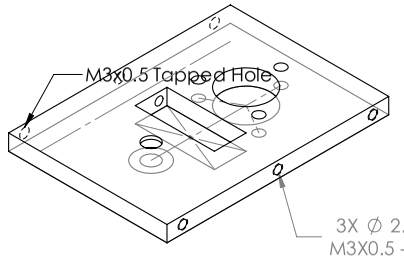

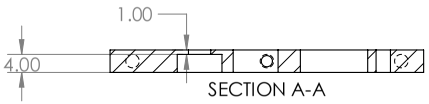

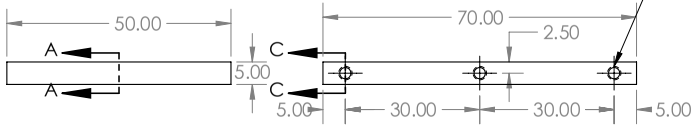

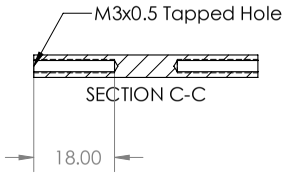

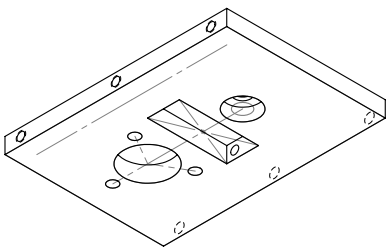

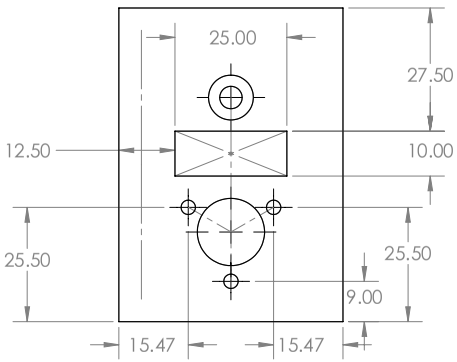

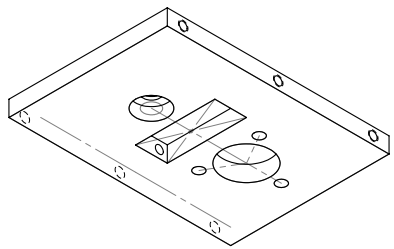

UNLESS OTHERWISE SPECIFIED: DIMENSIONS ARE IN MILLIMETERS SURFACE FINISH: TOLERANCES: LINEAR: ANGULAR:		FINISH:			DEBURR AND BREAK SHARP EDGES	DO NOT SCALE DRAWING	REVISION
	NAME	SIGNATURE	DATE			TITLE:	
DRAWN							
CHK'D							
APPV'D							
MFG							
Q.A				MATERIAL:		DWG NO. plate topp	A3
				WEIGHT:		SCALE:1:1	SHEET 1 OF 1

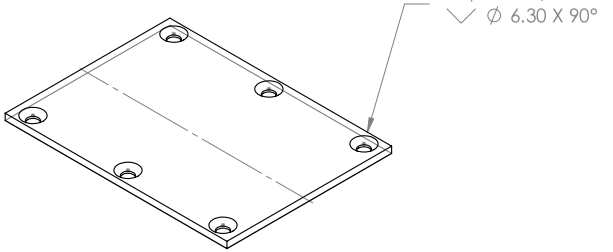

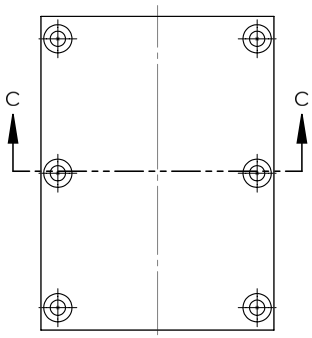

SECTION C-C

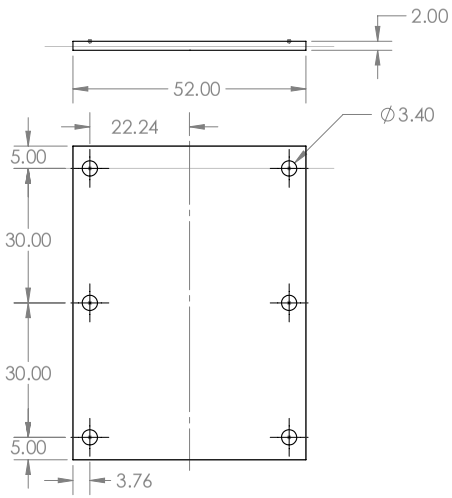

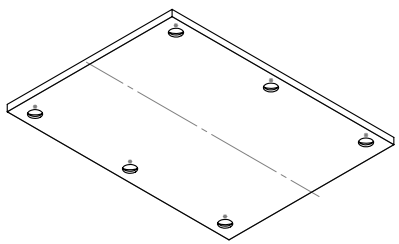

UNLESS OTHERWISE SPECIFIED: DIMENSIONS ARE IN MILLIMETERS SURFACE FINISH: TOLERANCES: LINEAR: ANGULAR:		FINISH:				DEBURR AND BREAK SHARP EDGES	DO NOT SCALE DRAWING / REVISION
	NAME	SIGNATURE	DATE				TITLE:
DRAWN							
CHK'D							
APPV'D							
MFG							
Q.A				MATERIAL:			DWG NO. plate sidevegg / A3
				WEIGHT:			SCALE:1:1 / SHEET 1 OF 1

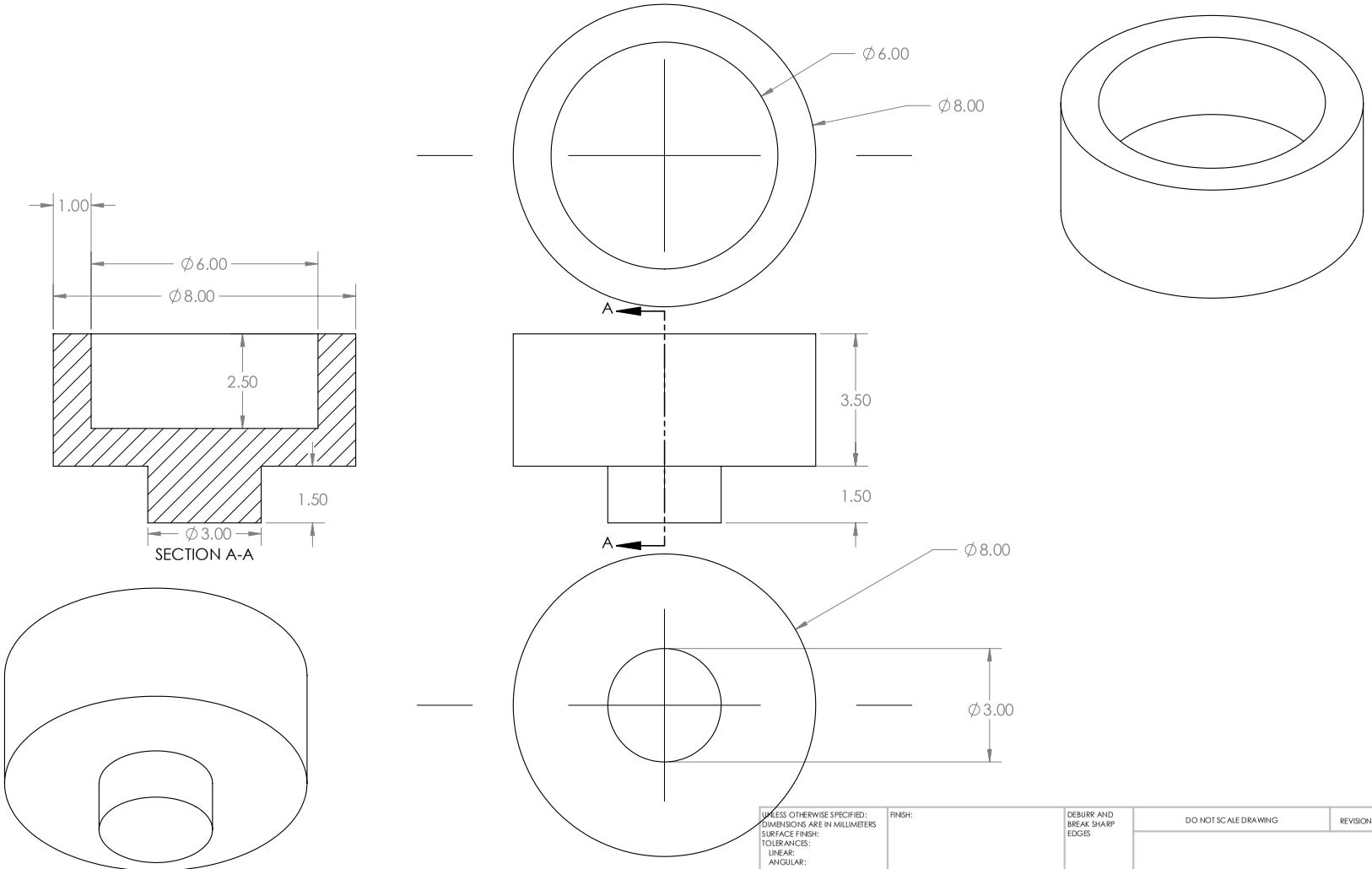

UNLESS OTHERWISE SPECIFIED: DIMENSIONS ARE IN MILLIMETERS SURFACE FINISH: TOLERANCES: LINEAR: ANGULAR:	FINISH:		DEBURR AND BREAK SHARP EDGES	DO NOT SCALE DRAWING	REVISION	
	NAME	SIGNATURE	DATE			TITLE:
DRAWN						
CHK'D						
APPV'D						
MFG						
Q.A				MATERIAL:	DWG NO. magnetkopp	A3
				WEIGHT:	SCALE:10:1	SHEET 1 OF 1